FEBS Letters 586 (2012) 2488–2493

FEBS Letters

journal homepage: www.FEBSLetters.org

RING finger palmitoylation of the endoplasmic reticulum Gp78 E3 ubiquitin ligase

Maria Fairbank [a], Kun Huang [b,c], Alaa El-Husseini [b,1], Ivan R. Nabi [a,*]

[a] University of British Columbia, Department of Cellular and Physiological Sciences, Vancouver, British Columbia, Canada
[b] University of British Columbia, Department of Psychiatry and Brain Research Center, Vancouver, British Columbia, Canada
[c] University of British Columbia, Centre for Molecular Medicine and Therapeutics, Vancouver, British Columbia, Canada

ARTICLE INFO

Article history:
Received 10 April 2012
Revised 30 May 2012
Accepted 1 June 2012
Available online 21 June 2012

Edited by Noboru Mizushima

Keywords:
Gp78
E3 ubiquitin ligase
ERAD
S-palmitoylation
Trafficking
Endoplasmic reticulum

ABSTRACT

Gp78 is an E3 ubiquitin ligase within the endoplasmic reticulum-associated degradation pathway. We show that Flag-tagged gp78 undergoes sulfhydryl cysteine palmitoylation (S-palmitoylation) within the RING finger motif, responsible for its ubiquitin ligase activity. Screening of 19 palmitoyl acyl transferases (PATs) identified five that increased gp78 RING finger palmitoylation. Endoplasmic reticulum (ER)-localized Myc-DHHC6 overexpression promoted the peripheral ER distribution of Flag-gp78 while RING finger mutation and the palmitoylation inhibitor 2-bromopalmitate restricted gp78 to the central ER. Palmitoylation of RING finger cysteines therefore regulates gp78 distribution to the peripheral ER.

1. Introduction

Gp78 is a critical E3 ubiquitin ligase in the endoplasmic reticulum-associated degradation (ERAD) pathway that targets multiple proteins for degradation via addition of polyubiquitin chains for proteasome-dependent degradation [1]. The gp78 RING finger motif consists of a conserved series of cysteine and histidine residues that bind two zinc atoms in a unique 'cross-brace' arrangement. The specific structural conformation of the RING finger is a critical component of its ubiquitin ligase function [2]. Here, we report, for the first time, RING finger palmitoylation of an endoplasmic reticulum (ER) localized ubiquitin ligase, gp78. Sulfhydryl cysteine palmitoylation (or S-palmitoylation), the addition of palmitate (a 16-carbon saturated fatty acid) to specific cysteine residues via a thioester linkage, has been identified in various proteins including many neuronal proteins and G protein-coupled receptors (GPCRs) [3–5]. Palmitoylation, similar to phosphorylation, is a dynamic, reversible post-translational modification that regulates cellular responses by altering receptor trafficking, function and stability [6,7]. Palmitoylation of gp78 is shown here to induce its distribution to the peripheral ER defining a novel post-translational modification able to control the ER distribution of this key ubiquitin ligase in ERAD.

2. Materials and methods

2.1. Plasmids and constructs

Mouse Flag-gp78 [8], 19 DHHC expression plasmids [9] and GFP-Sec61β [10] are as previously described. The Flag-gp78 N-terminal transmembrane domain construct was generated by substituting L330 for a stop codon. All point mutations in Flag-gp78 (C88/89A, C100A, C145A, C161A, C194/195A, C200/201A, C337/340A, C352S, C360A, C371/374A) were generated using the Quickchange Mutagenesis Kit (Stratagene) and sequences of mutated DNA constructs were confirmed.

2.2. Antibodies

Anti-Flag M2 and anti-calnexin were purchased from Sigma and anti-Myc (clone 4A6) from Millipore. The rat IgM 3F3A monoclonal antibody against gp78 is described in [11]. Fluorescently conjugated secondary antibodies for immunocytochemistry were purchased from Invitrogen. For immunoblotting experiments, HRP-conjugated secondary antibodies were purchased from Jackson Immunoresearch. For the Odyssey Infrared Imaging System (Li-COR Bioscience), anti-mouse IRDye 800 antibody was purchased from Rockland and streptavidin-Cy5 from Invitrogen.

* Corresponding author. Address: Department of Cellular and Physiological Sciences, Life Sciences Institute, University of British Columbia, 2350 Health Sciences Mall, Vancouver, BC, Canada V6T 1Z3.
E-mail address: irnabi@mail.ubc.ca (I.R. Nabi).
[1] Deceased.

0014-5793/$36.00
http://dx.doi.org/10.1016/j.febslet.2012.06.011

2.3. Cell culture and transfection

Cos7 cells were maintained in DMEM containing 10% fetal bovine serum (FBS, MediCorp.), and supplemented with 0.2 mM L-glutamine, 10 μg/ml penicillin, 10 μg/ml streptomycin, vitamins and non-essential amino acids (all supplements from Invitrogen). For transient transfection (24 h) of plasmid DNA into Cos7 cells, Effectene Transfection Reagent (Qiagen) was used as described by the manufacturer. 2-Bromohexadecanoic acid (2-bromopalmitate (2-BP)) (Fluka) was used as described in the figure legends.

2.4. Immunoprecipitation, immunoblotting and immunofluorescence

Anti-Flag immunoprecipitation, immunoblotting and immunofluorescence labeling were as previously described [12]. For immunoblot analysis, results are expressed as Mean ± S.E.M. and statistical comparisons between groups were performed (GraphPad PRISM) by using oneway analysis of variance (ANOVA) followed by Tukey's multiple comparison tests or a two-tailed unpaired Student's *t* test (Fig. 3D). For fluorescence quantification experiments, ImagePro analysis software (Media Cybernetics) was used to determine colocalization between two proteins by Pearson's coefficient or by the percentage of Flag-gp78 localized in the central ER [13].

2.5. Acyl-Biotin Exchange chemistry (or Biotin-BMCC labeling)

This method was adapted from [14]. During the anti-Flag immunoprecipitation, supernatants were supplemented with 50 mM N-ethylmaleimide (NEM, Sigma). Each sample was divided into two portions for treatment with or without (as a control) 1 M hydroxylamine (HAM, Sigma) at pH 7.4 for 1 h at room temperature. Subsequently, all samples were incubated with 1 μM EZ-link Biotin-BMCC (biotin-N-(6-(biotinamido)hexyl)-3′-(2′-pyridyldithio)-propionamide biotinylation; Fisher Scientific) at pH 6.2 for 1 h at 4 °C to label reactive cysteine residues. Following SDS–PAGE and transfer to PVDF membranes, the Odyssey Infrared Imaging System was used to visualize Biotin-BMCC-labeled Flag-gp78 with streptavidin-Cy5 and total Flag-gp78 with anti-Flag antibody and anti-mouse IRDye 800 antibody.

3. Results

3.1. Gp78 is palmitoylated in the RING finger motif

To determine whether gp78 undergoes cysteine palmitoylation or S-palmitoylation, we used Acyl-Biotin Exchange chemistry, also referred to as Biotin-BMCC labeling [14]. The Biotin-BMCC method labeled full-length Flag-gp78 (FL) and full-length Flag-gp78 lacking N-terminal cysteines (FL ΔC TMD) (Fig. 1A and B). Furthermore, a truncated gp78 construct containing only the N-terminal transmembrane domains (TMD) was not labeled (Fig. 1A and C). This suggests that S-palmitoylation is localized to C-terminal cysteines, all found within the RING finger domain (Fig. 2A). Mutation of individual cysteines or combinations of two or three cysteines within the RING finger all significantly reduced gp78 palmitoylation (Fig. 2B and D). However, the palmitoylation signal was only lost when every RING finger cysteine was substituted with an alanine (Fig. 2C and D), suggesting that all RING finger cysteines show a degree of affinity for S-palmitoylation.

We then investigated modulation of gp78 palmitoylation by exogenously co-expressing palmitoyl acyl transferases (PATs), also known as DHHC enzymes that mediate the addition of palmitoyl CoA to proteins [15]. Using Biotin-BMCC labeling, we screened 19 Myc-DHHC enzymes and identified 5 DHHC enzymes (DHHC2, DHHC6, DHHC11, DHHC13 (HIP14L) and DHHC24) that increased gp78 palmitoylation by at least 1.5-fold (Fig. 3A and B). In Cos7 cells, these DHHC enzymes vary in their subcellular distributions: DHHC2 localizes mostly to the plasma membrane, DHHC 13 is predominantly found in the Golgi, while DHHC6, DHHC 11 and DHHC24 are all expressed in the ER (Fig. S1). We further explored the role of ER-localized DHHC6. In the absence of all RING finger cysteines, Flag-gp78 palmitoylation was not significantly enhanced by DHHC6 (Fig. 3C), suggesting that DHHC6 selectively targets palmitoylation in the RING finger domain. Similarly, gp78 palmitoylation was reduced by 40% following a 6 h treatment with a

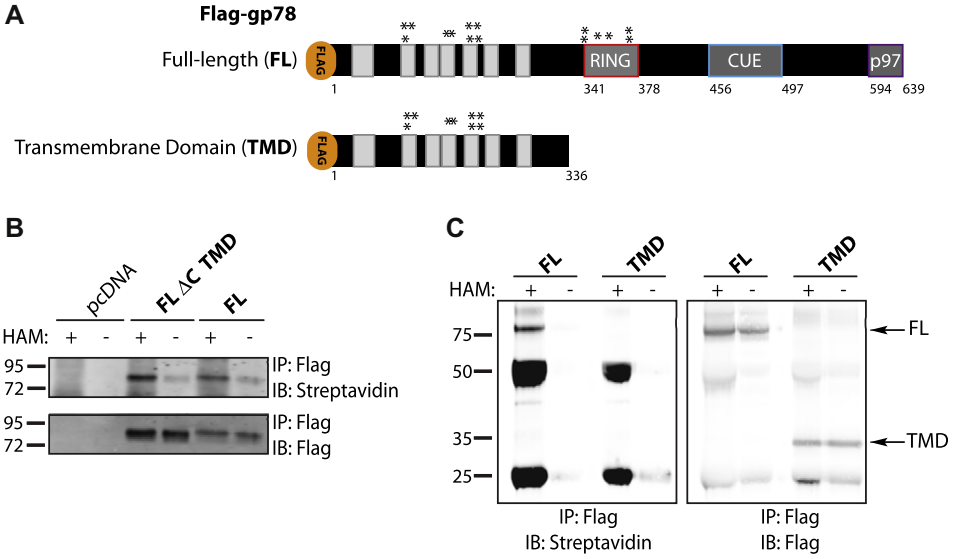

Fig. 1. Gp78 is S-palmitoylated in the C-terminal domain. (A) Schematic of mouse gp78 constructs used in the Biotin-BMCC labeling (* identify the location of all cysteine residues). (B and C) Gp78 constructs (FL: Full-length Flag-gp78; FL ΔC TMD: Full-length Flag-gp78 absent of all nine cysteines in the transmembrane domain; TMD: truncated N-terminal Flag-gp78 transmembrane domain) were tested for palmitoylation. Immunoblots were probed with streptavidin-Cy5 (to detect Biotin-BMCC-labeled proteins) and anti-Flag antibody followed by IRDye 800 mouse antibody (to detect Flag-tagged total proteins), and imaged with the Odyssey Infrared Imaging System. Data are representative of three independent experiments.

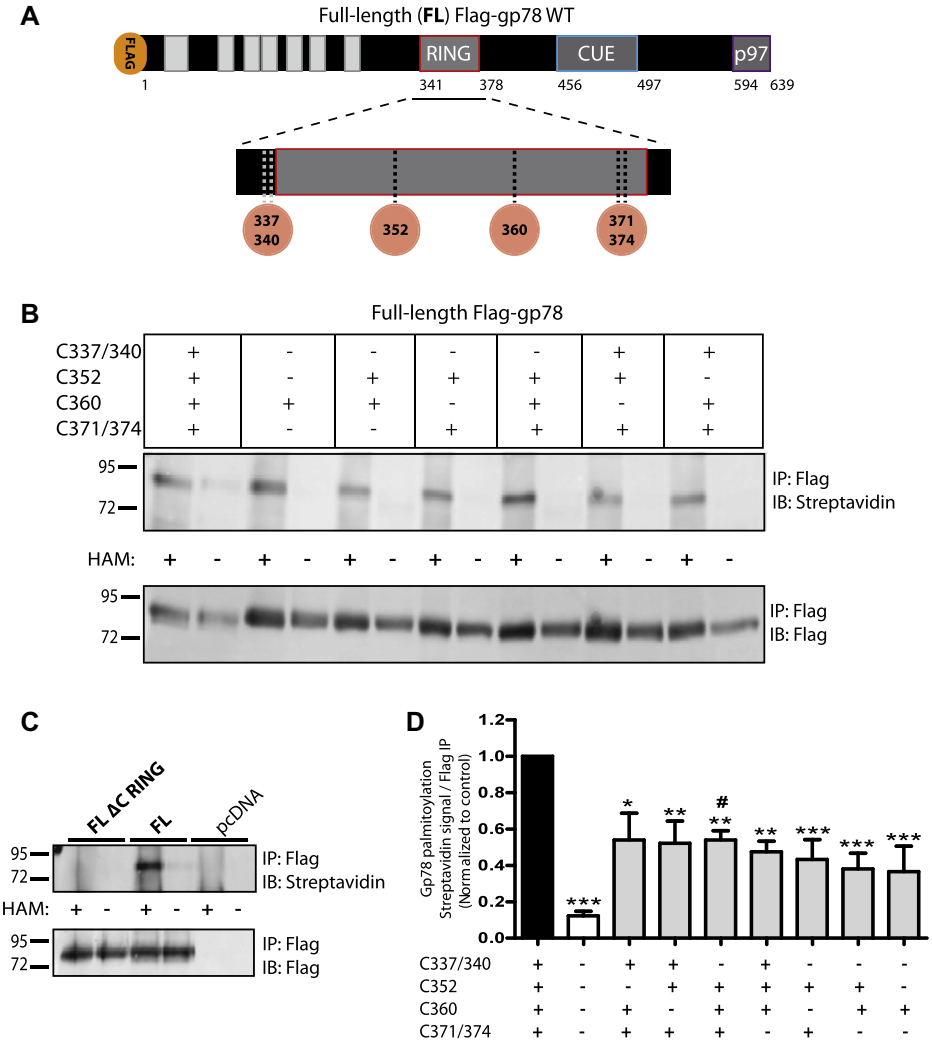

Fig. 2. Gp78 is S-palmitoylated on cysteines within the C-terminal RING finger domain. (A) The C-terminal of gp78 contains six cysteines all located within a RING finger motif that is responsible for its ubiquitin ligase activity. Additional domains include an ubiquitin binding CUE motif and a p97/VCP binding domain. (B and C) Using site-directed mutagenesis, cysteines in the RING finger motif were systematically substituted for alanines (C337, C340, C360, C371, C374) or a serine (C352) in full-length Flag-gp78, generating a cysteine-free RING finger mutant (ΔC RING). Eight mutant constructs were tested for palmitoylation using Biotin-BMCC labeling. (D) Band densities were first normalized with respect to protein levels from anti-Flag immunoblots, and then each mutant was normalized to wild-type Flag-gp78 (control). (Mean ± S.E.M.; $^{*}P < 0.05$, $^{**}P < 0.01$, $^{***}P < 0.001$ compared to wild-type. $^{\#}P < 0.05$ compared to the cysteine-free RING finger mutant). Data are representative of four to six experiments.

broad inhibitor of palmitoylation, 2-bromopalmitate (2-BP) (Fig. 3D), reinforcing the specificity of the S-palmitoylation signal detected in the Biotin-BMCC labeling.

3.2. Gp78 palmitoylation regulates its ER distribution

Flag-gp78 is localized to both the peripheral and central ER and its ubiquitin ligase activity has recently been shown to be initiated in the peripheral ER [13]. Expression of Myc-DHHC6 reduced central ER labeling of Flag-gp78, defined by the central ER marker GFP-Sec61β, relative to the periphery of the cell. Peripheral Flag-gp78 redistribution was not observed with Myc-DHHC 19 (Fig. 4), an ER-localized DHHC enzyme that does not modulate gp78 palmitoylation (Fig. 3B). As previously reported for the gp78 C352S RING finger mutation [13], all RING finger Flag-gp78 mutants show increased colocalization with calnexin (Fig. S2) that codistributes extensively with central ER-localized GFP-Sec61β (data not shown).

Distribution of the cysteine-free RING finger Flag-gp78 mutant (ΔC RING) to the central ER was not affected by expression of Myc-DHHC6 (Fig. 4). Similarly, following 2-BP treatment, Flag-gp78 accumulated in the GFP-Sec61β-defined central ER and the enhanced peripheral distribution of Flag-gp78 in the presence of Myc-DHHC6 was reversed (Fig. S3). Peripheral ER-localized Flag-gp78 colocalized extensively with 3F3 A anti-gp78 labeling (Fig. 5), a marker for the peripheral, smooth ER [16,17]. Confocal image analysis showed that all 5 DHHC enzymes that target gp78 promoted a redistribution of Flag-gp78 to the peripheral ER (data not shown). Gp78 palmitoylation therefore promotes its distribution to the peripheral ER.

4. Discussion

This study describes, for the first time, palmitoylation of the RING finger motif of an E3 ubiquitin ligase. Gp78 is an E3 ubiquitin ligase in ERAD that can be palmitoylated by various PATs, including ER-localized DHHC6. We show that palmitoylation promotes the distribution of gp78 to the peripheral ER, the site of initiation of gp78 ubiquitin ligase activity [13]. As a result, palmitoylation of the gp78 RING finger motif may affect gp78 substrate degradation in the ERAD pathway by disrupting the RING finger motif but also by regulating gp78 ER distribution.

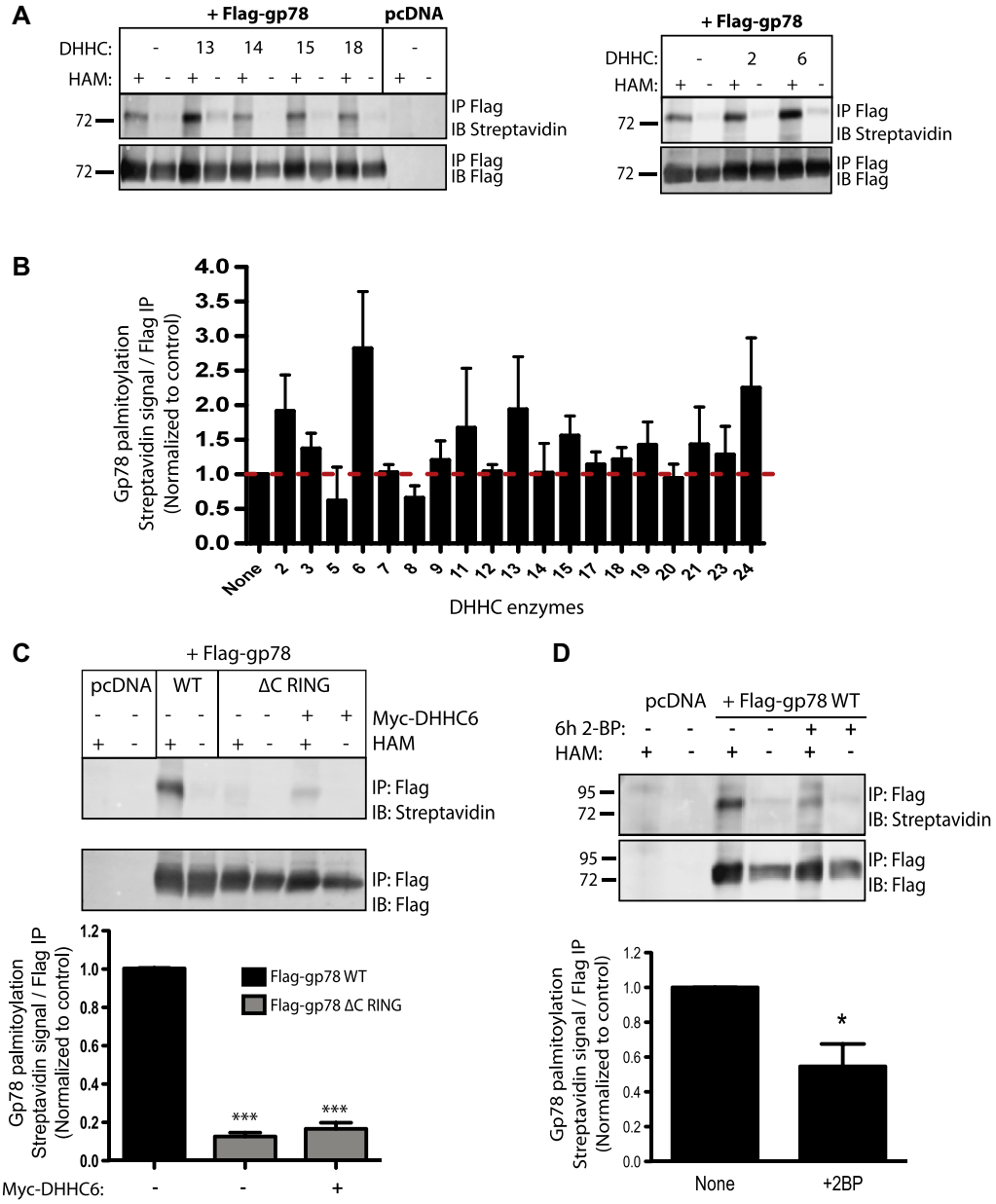

Fig. 3. S-palmitoylation by several DHHC enzymes of gp78 within the RING finger motif. (A and B) Cos7 cells were transiently transfected with either full-length Flag-gp78 alone or with a Myc-DHHC enzyme. Following anti-Flag immunoprecipitation, palmitoylation of Flag-gp78 was determined by Biotin-BMCC labeling. Quantification of gp78 palmitoylation by individual DHHC enzymes as labeled by streptavidin-Cy5 was first normalized to protein levels from anti-Flag immunoblots, and then to wild-type Flag-gp78 alone (control). (C) Cos7 cells were transfected with the cysteine-free RING finger mutant (Flag-gp78 ΔC RING), in the presence and absence of Myc-DHHC6. Following anti-Flag immunoprecipitation and Biotin-BMCC labeling, the Flag-gp78 ΔC RING palmitoylation signal was compared to wild-type Flag-gp78 alone (Mean ± S.E.M.; $^{***}P < 0.001$). (D) Anti-Flag immunoprecipitation and Biotin-BMCC labeling were used to determine the level of Flag-gp78 palmitoylation in Cos7 cells after a 6 h treatment with a solvent (DMSO) or a broad inhibitor of palmitoylation, 2-bromopalmitate (100 nM 2-BP). Quantification of gp78 palmitoylation was first normalized to protein levels from anti-Flag immunoblots, and then to wild-type Flag-gp78 alone (Mean ± S.E.M.; $^{*}P < 0.05$). Data are representative of three to five experiments.

Using site-directed mutagenesis, we failed to identify a preferentially palmitoylated RING finger cysteine since all mutants displayed a 40–60% decrease in palmitoylation, with the exception of the cysteine-free RING finger mutant (Fig. 2). These data reinforce the concept that palmitoylation can occur on more than one cysteine residue within membrane proteins, as seen for several AMPA receptor subunits and the NMD A receptor [18,19]. A RING finger mutant that contains an inhibitory point mutation in the third cysteine (C352S) showed significantly reduced palmitoylation levels (Fig. 2) and a reduced ability to generate polyubiquitylated substrates when co-transfected with HA-tagged ubiquitin [13]. Mutation of other RING finger cysteines will likely have a similar effect, as suggested by the similar central ER distribution of various RING finger cysteine mutants (Fig. S2). The specific relationship between RING finger palmitoylation and gp78 ubiquitin ligase activity remains to be determined.

Screening analysis of 23 mammalian DHHC enzymes has demonstrated that a number of substrates are differentially palmitoylated by specific DHHC enzymes [20,21]. This is consistent with our observation that 5 DHHC enzymes (DHHC2, DHHC6, DHHC11, DHHC 13 and DHHC24) palmitoylate Flag-gp78 (Fig. 3). Overall, these data are indicative of both specificity and redundancy

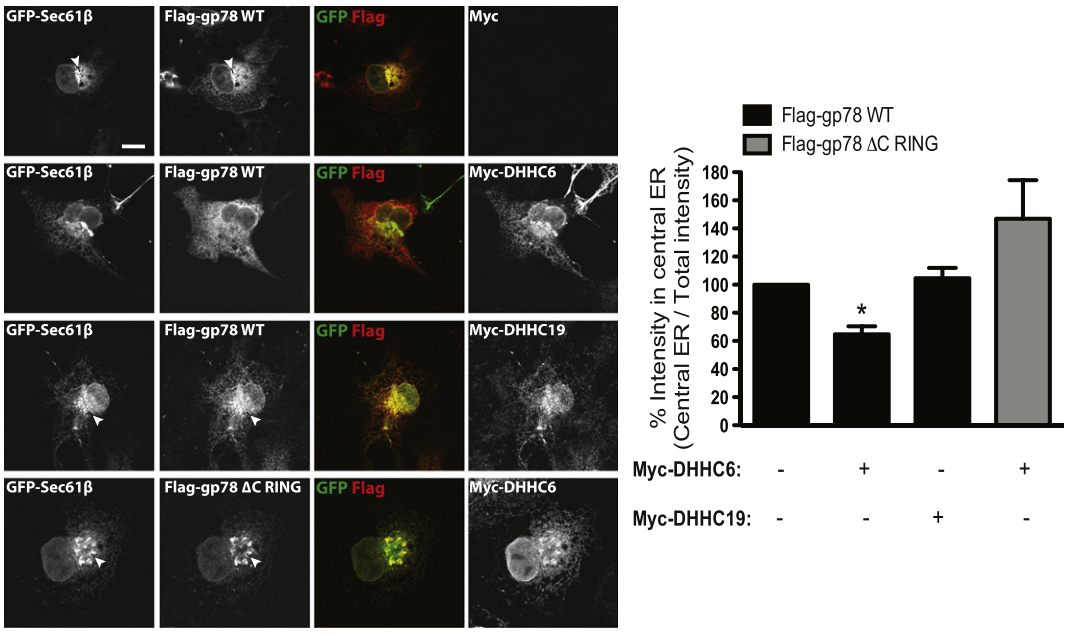

Fig. 4. DHHC6-mediated gp78 RING finger palmitoylation enhances its peripheral ER distribution. Cos7 cells were transiently transfected with a central ER marker (GFP-Sec61β) and either Flag-gp78 wild-type (WT) or the cysteine-free RING finger mutant (Flag-gp78 ΔC RING), alone or in the presence of Myc-DHHC6 or Myc-DHHC 19, fixed and labeled with anti-Flag and anti-Myc and imaged by confocal microscopy. The percent intensity of Flag-gp78 (with and without DHHC enzyme) in the central ER was determined by using GFP-Sec61β as a mask (Mean ± S.E.M.; $^{*}P < 0.05$ compared to Flag-gp78). Arrows indicate protein accumulation in the central ER. 22–42 cells per condition were imaged from five to six independent experiments. Scale bar = 20 μm.

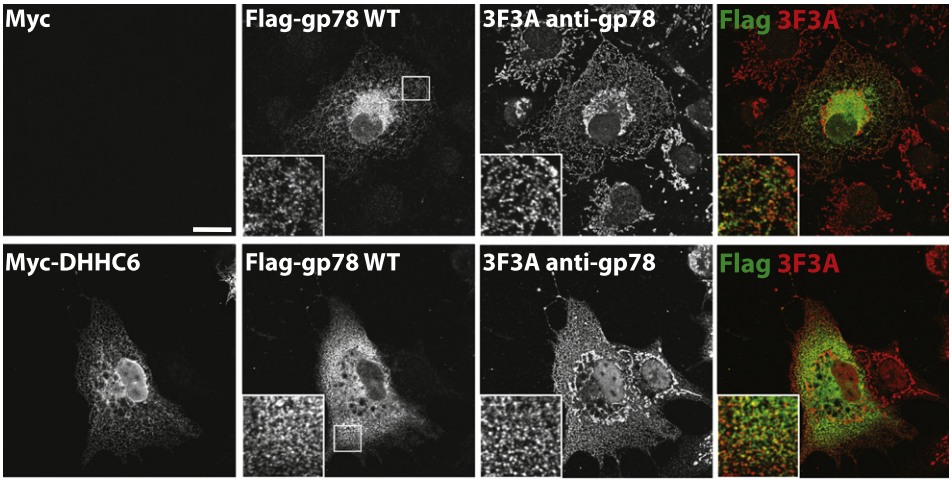

Fig. 5. Gp78 colocalizes with the 3F3A peripheral, smooth ER marker. Cos7 cells were transiently transfected with Flag-gp78 WT in the presence and absence of Myc-DHHC6, fixed and labeled with anti-Flag, anti-Myc and 3F3 A anti-gp78 antibodies and imaged by confocal microscopy. 18–24 cells per condition were imaged from six independent experiments. Scale bar = 20 μm; zoom scale bar = 0.3 μm.

amongst DHHC enzymes that may have functional relevance in light of the differential expression of DHHC enzymes in various tissue types [9].

By electron microscopy, the ER can be separated into smooth and rough, ribosome studded domains. These have more recently been shown to correspond, in cultured cells, to the peripheral, tubular ER and central, saccular ER [22]. However, mechanisms that control protein distribution between these domains remain poorly understood. We show that Ring finger palmitoylation targets gp78 to the peripheral ER (Figs. 4 and 5), the site of initiation of gp78 ubiquitin ligase activity [13]. Mutation of RING finger cysteines (Fig. S2) and inhibition of palmitoylation with 2-BP (Fig. S3) both restrict gp78 to the central ER. By disrupting its RING finger domain and promoting gp78 peripheral ER distribution, palmitoylation may therefore represent a mechanism to regulate and localize gp78 ubiquitin ligase activity to the peripheral ER [12,13].

Since S-palmitoylation is highly dynamic, RING finger palmitoylation may represent a novel mechanism for the regulation of the activity, stability and cellular distribution of this ERAD-associated ubiquitin ligase. Similarly, RING finger palmitoylation could have significant implications for the activity of other E3 ubiquitin ligases and their ERAD substrates, ultimately affecting homeostatic and pathological processes. Here, we propose that by regulating RING finger integrity and gp78 ER distribution, palmitoylation may impact on its E3 ubiquitin ligase function in ERAD. Whether RING

finger palmitoylation is gp78-specific or a general mechanism to control the activity of RING finger ubiquitin ligases remains to be determined.

Acknowledgements

This work was initiated as a collaboration with Alaa El-Husseini, since deceased, and we are grateful for his insight and support. We also thank Michael Hayden for his help in completing this study. We thank members in Dr. Nabi's laboratory in particular Pascal St-Pierre for providing the Flag-gp78 C352S RING finger mutant. Supported by the Canadian Institutes for Health Research (CIHR MT-15132; IRN) and a Michael Smith Foundation for Health Research Scholarship to M.F.

Appendix A. Supplementary data

Supplementary data associated with this article can be found, in the online version, at http://dx.doi.org/10.1016/j.febslet.2012.06.011.

References

[1] Christianson, J.C. et al. (2012) Defining human ERAD networks through an integrative mapping strategy. Nat. Cell Biol. 14, 93–105.
[2] Freemont, P.S. (2000) RING for destruction? Curr. Biol. 10, R84–R87.
[3] Resh, M.D. (2006) Palmitoylation of ligands, receptors, and intracellular signaling molecules. Sci. STKE 2006, re14.
[4] el-Husseini Ael, D. and Bredt, D.S. (2002) Protein palmitoylation: a regulator of neuronal development and function. Nat. Rev. Neurosci. 3, 791–802.
[5] Qanbar, R. and Bouvier, M. (2003) Role of palmitoylation/depalmitoylation reactions in G-protein-coupled receptor function. Pharmacol. Ther. 97, 1–33.
[6] Huang, K. and El-Husseini, A. (2005) Modulation of neuronal protein trafficking and function by palmitoylation. Curr. Opin. Neurobiol. 15, 527–535.
[7] Linder, M.E. and Deschenes, R.J. (2007) Palmitoylation: policing protein stability and traffic. Nat. Rev. Mol. Cell Biol. 8, 74–84.
[8] Registre, M., Goetz, J.G., St Pierre, P., Pang, H., Lagace, M., Bouvier, M., Le, P.U. and Nabi, I.R. (2004) The gene product of the gp78/AMFR ubiquitin E3 ligase cDNA is selectively recognized by the 3F3A antibody within a subdomain of the endoplasmic reticulum. Biochem. Biophys. Res. Commun. 320, 1316–1322.
[9] Ohno, Y., Kihara, A., Sano, T. and Igarashi, Y. (2006) Intracellular localization and tissue-specific distribution of human and yeast DHHC cysteine-rich domain-containing proteins. Biochim. Biophys. Acta 1761, 474–483.
[10] Voeltz, G.K., Prinz, W.A., Shibata, Y., Rist, J.M. and Rapoport, T.A. (2006) A class of membrane proteins shaping the tubular endoplasmic reticulum. Cell 124, 573–586.
[11] Nabi, I.R., Watanabe, H. and Raz, A. (1990) Identification of B16-F1 melanoma autocrine motility-like factor receptor. Cancer Res. 50, 409–414.
[12] St Pierre, P. and Nabi, I.R. (2012) The Gp78 ubiquitin ligase: probing endoplasmic reticulum complexity. Protoplasma 249 (Suppl 1), S11–S18.
[13] St-Pierre, P., Dang, T., Joshi, B. and Nabi, I.R. (2012) Peripheral endoplasmic reticulum localization of the Gp78 ubiquitin ligase activity. J. Cell Sci. 125, 1727–1737.
[14] Drisdel, R.C. and Green, W.N. (2004) Labeling and quantifying sites of protein palmitoylation. Biotechniques 36, 276–285.
[15] Iwanaga, T., Tsutsumi, R., Noritake, J., Fukata, Y. and Fukata, M. (2009) Dynamic protein palmitoylation in cellular signaling. Prog. Lipid Res. 48, 117–127.
[16] Benlimame, N., Simard, D. and Nabi, I.R. (1995) Autocrine motility factor receptor is a marker for a distinct membranous tubular organelle. J. Cell Biol. 129, 459–471.
[17] Benlimame, N., Le, P.U. and Nabi, I.R. (1998) Localization of autocrine motility factor receptor to caveolae and clathrin-independent internalization of its ligand to smooth endoplasmic reticulum. Mol. Biol. Cell 9, 1773–1786.
[18] Hayashi, T., Rumbaugh, G. and Huganir, R.L. (2005) Differential regulation of AMP A receptor subunit trafficking by palmitoylation of two distinct sites. Neuron 47, 709–723.
[19] Hayashi, T., Thomas, G.M. and Huganir, R.L. (2009) Dual palmitoylation of NR2 subunits regulates NMDA receptor trafficking. Neuron 64, 213–226.
[20] Fang, C., Deng, L., Keller, C.A., Fukata, M., Fukata, Y., Chen, G. and Luscher, B. (2006) GODZ-mediated palmitoylation of GAB A(A) receptors is required for normal assembly and function of GABAergic inhibitory synapses. J. Neurosci. 26, 12758–12768.
[21] Huang, K., Kang, M.H., Askew, C., Kang, R., Sanders, S.S., Wan, J., Davis, N.G. and Hayden, M.R. (2010) Palmitoylation and function of glial glutamate transporter-1 is reduced in the YAC128 mouse model of Huntington disease. Neurobiol. Dis. 40, 207–215.
[22] Shibata, Y., Shemesh, T., Prinz, W.A., Palazzo, A.F., Kozlov, M.M. and Rapoport, T.A. (2010) Mechanisms determining the morphology of the peripheral ER. Cell 143, 774–788.